

## Memristive adaptive filters

T. Driscoll,<sup>1,a)</sup> J. Quinn,<sup>1</sup> S. Klein,<sup>1</sup> H. T. Kim,<sup>2</sup> B. J. Kim,<sup>2</sup> Yu. V. Pershin,<sup>3</sup> M. Di Ventra,<sup>1</sup> and D. N. Basov<sup>1</sup>

<sup>1</sup>Department of Physics, University of California–San Diego, La Jolla, California 92093, USA

<sup>2</sup>Metal-Insulator Transition Laboratory, Electronics and Telecommunications Research Institute (ETRI), Daejeon 305-350, Republic of Korea

<sup>3</sup>Department of Physics and Astronomy and USC NanoCenter, University of South Carolina, Columbia, South Carolina 29208, USA

(Received 11 June 2010; accepted 11 August 2010; published online 1 September 2010)

Using the memristive properties of vanadium dioxide, we experimentally demonstrate an adaptive filter by placing a memristor into an  $LC$  contour. This circuit reacts to the application of select frequency signals by sharpening the quality factor of its resonant response, and thus “learns” according to the input waveform. The proposed circuit employs only analog passive elements, and may find applications in biologically inspired processing and information storage. We also extend the learning-circuit framework mathematically to include memory-reactive elements, such as memcapacitors and meminductors, and show how this expands the functionality of adaptive memory filters. © 2010 American Institute of Physics. [doi:10.1063/1.3485060]

Recent experimental results involving nonlinear resistance devices have generated interest in a specific class of memory-circuit-elements known as memristive (short for memory-resistive) systems. Memristive effects have been observed experimentally for decades.<sup>1–4</sup> However, the recent description of experimental results<sup>5,6</sup> within the mathematical framework of memristance,<sup>7,8</sup> and memory-reactance (memcapacitance and meminductance<sup>9</sup>) has provided a foundation in which to understand and interpret these results. Recent interest has also been driven by the realization that such devices are likely to have a significant and broad impact in electronics.<sup>10</sup> In particular, it is believed that memristive systems have the potential to revolutionize both information processing and nonvolatile memory storage.<sup>11–13</sup> Much of the innovation so far has centered on using memory mechanisms to improve upon existing digital techniques. For example, memristors offer the tantalizing possibility of unifying the now-separate nonvolatile memory (hard-disk) and computation (CPU) areas of traditional computers.<sup>14,15</sup> However, memristive elements also offer advanced analog functionalities.<sup>16,17</sup> For instance, memristive systems are

stable at essentially any point between following two limiting cases: the minimum low resistance and maximum high resistance—limits imposed by the physics of the specific material base. In this letter, we use the analog functionality of memory-circuit elements to demonstrate real-time-responsive adaptive (“learning”) filters. Such adaptive memory filters have been considered before<sup>18</sup> to model the surprisingly complex learning behavior observed in amoebas.

Using a vanadium dioxide ( $\text{VO}_2$ ) memristor,<sup>19</sup> we experimentally demonstrate the adaptive filter functionality originally simulated in Ref. 18. We construct the simple  $R_mLC$  bandpass filter shown in Fig. 1(a) by adding a  $\text{VO}_2$  memristive device ( $R_m$ ) in series with an external capacitor ( $C$ ) and inductor ( $L$ ). The schematic in Fig. 1(a) also includes a memory-capacitance  $C_m$  associated with  $\text{VO}_2$  that was observed in Ref. 20. Here, however,  $C_m$  plays a minor role in the behavior of our experimental circuit due to  $C_m \ll C$ . To maximize  $\text{VO}_2$  memristance, the device is heated to a steady-state temperature of 339.80 K. The details of this

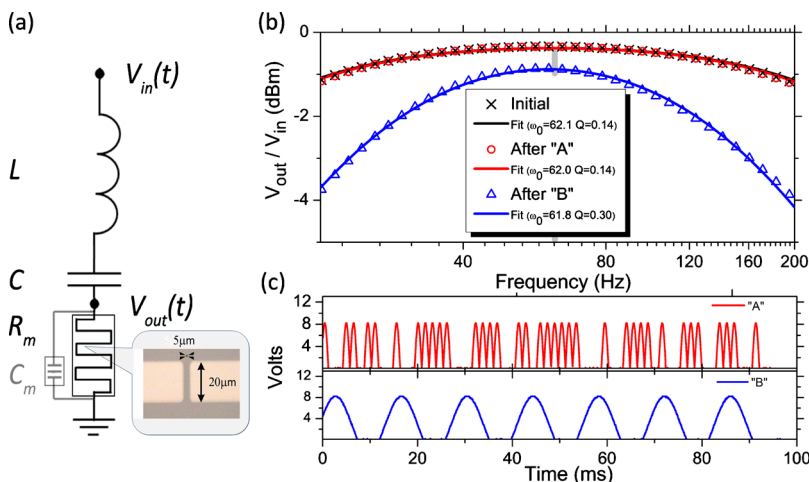


FIG. 1. (Color online) (a). Schematic for  $R_mLC$  adaptive memory filter. Memory capacitance ( $C_m$ ) present in  $\text{VO}_2$  is also drawn, although in our setup  $C_m \ll C$  which masks any memory capacitive effects. The inset shows an optical photograph of the two-terminal device used, a  $5 \mu\text{m} \times 20 \mu\text{m}$   $\text{VO}_2$  region lithographically defined by gold contacts. (b) Small-signal (10 mV) transfer function ( $V_{\text{out}}/V_{\text{in}}$ ) for the adaptive filter plotted before and after off-resonance “A” and on-resonance “B” pulses. Solid lines are  $RLC$  bandpass-filter fit to data, which generates the  $\omega_0$  and  $Q$  values in the legend. Pulse sequence B has a significant training effect on the circuit, while A has little or no effect. (c) Time series of the off-resonance “A” sequence of pulses and on-resonance “B” sequence of pulses.

<sup>a)</sup>Electronic mail: tdriscol@physics.ucsd.edu.

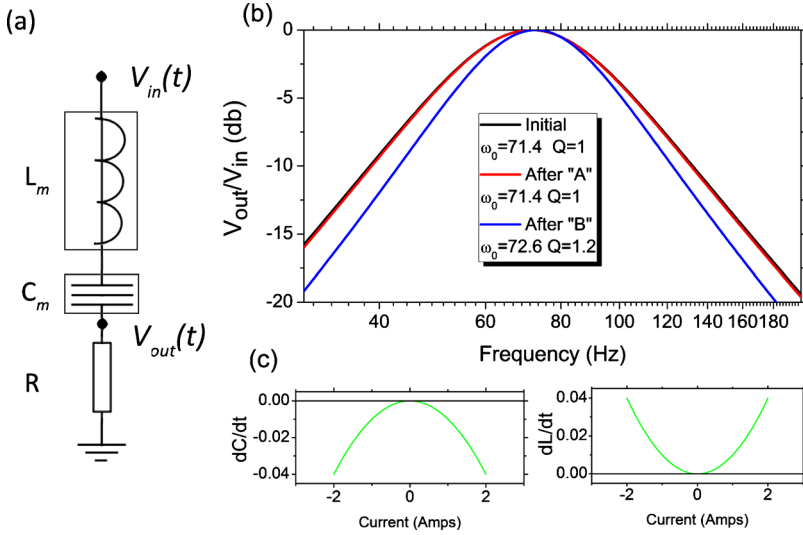


FIG. 2. (Color online) (a). Schematic for proposed  $RL_mC_m$  adaptive memory filter. (b) Small-signal (10 mV) transfer function ( $V_{out}/V_{in}$ ) for the adaptive filter plotted before and after the same “A” and “B” pulse sequences used in Fig. 1.  $C_m$  and  $L_m$  are designed to evolve in response to current as shown in (c). As before, pulse sequence B has a significant training effect on the circuit, while A has little or no effect. In this  $RC_mL_m$  configuration however, the  $V_{out}/V_{in}$  at the peak of the bandpass is constant.

temperature bias approach are described in our previous work using  $VO_2$  memory structure.<sup>19,20</sup> The low-voltage (10 mV) transfer function of the filter ( $V_{out}/V_{in}$ ) is probed using a network analyzer (Stanford Research System 785). The initial transfer function, before any applied input signals, is plotted in Fig. 1(b) (black symbols: “initial”). The filter is then subjected to one of two series of pulses (using a HP 33120A function generator), designed to be either on or off resonance. The frequency and periodicity differences in the two waveforms are selected such that the two contain the same total power input to the memristor. These pulses waveforms are shown in Fig. 1(c), labeled “A” (off-resonance) and “B” (on-resonance), and five sequential repetitions of the waveform are used in each case. After each pulse sequence, the filter transfer function is probed again. We observe that pulse sequence A, the off-resonant sequence, causes almost no change from the initial filter state [Fig. 1(b) red symbols]. Sequence B, however, has a visible effect, showing a sharpening of the bandpass filter [Fig. 1(b) blue symbols]. In both cases, we have checked after the pulse sequences that the transfer function is stable, and exhibits no observable change for 5 min. In previous work we have found such  $VO_2$  devices subjected to similar pulse sequences to be stable for hours or longer.<sup>19</sup>

To understand the operation of this filter, we can look more closely at the behavior of a memristor best described by<sup>9</sup>

$$R_m = R_0 F(x_R), \quad \dot{x}_R = f(x_R, I_R, t), \quad (1)$$

where  $x$  are  $n$  variables that describe the internal state of the memristor. The function  $F(x_R)$  describes how the state-variables affect the macroscopic resistance, and  $f(x_R, I_R, t)$  is an  $n$ -dimensional vector function that describes the time-evolution of  $x_R$  in response to applied current through the memristor, which naturally follows the instantaneous voltage drop across the memristor  $V_{R_m}$ . These equations describe a nonlinear resistance with a current-dependent time-constant. When  $I_R=0$ ,  $\dot{x}_R=0$ , giving such devices a natural property of memory.<sup>11,13</sup> When placed in a filter like that of Fig. 1(a), the output response of the filter depends on the time-history of the voltage and frequency of applied signals. This is best seen in the bandpass equation

$$\frac{V_{R_m}}{V_{in}} = \frac{V_{out}}{V_{in}} = \frac{R_m}{\left[ \left( \frac{i}{C\omega} - iL\omega \right) + R_m \right]}. \quad (2)$$

Although in general, linear-time-invariant (LTI) analysis of memristive filter is not sufficient, here we can proceed with the understanding that any LTI description of the filter transfer function is valid only when  $\Delta t(\dot{x}_R/x_R) \approx 0$ . This condition is satisfied for small  $V_{R_m}$ , and so Eq. (2) correctly describes the low-voltage transfer functions plotted in Fig. 1. It also reveals that input signals with a strong component at the resonant frequency  $\omega_0 = (LC)^{-1/2}$  will place the greatest voltage across  $R_m$  and thus will strongly modify the memristor, whereas signals off-resonance will have less effect on the memristor.<sup>18</sup>

To quantify the observed changes in the transfer function, we fit each of the transfer-function data sets to a  $RLC$  bandpass equation,<sup>21</sup> extracting quality-factor  $Q = (1/R_m)\sqrt{(L/C)}$  and center-frequency  $\omega_0$  of the filter. These fits are the solid lines shown in Fig. 1(b). We see that the primary change to the on-resonance pulse B is a doubling of the  $Q$  of the filter with little change in  $\omega_0$ . Thus, this filter reacts to on-resonance signals by further sharpening its response, while it does not appreciably react to off-resonance signals.

One evident drawback of the present implementation utilizing memristance is that the transfer function is not self-normalizing. Even as  $Q$  sharpens, the absolute magnitude of the output at  $\omega_0$  decreases. Such non-normalized filters may be more difficult to work with in some cases. Therefore, as one possible avenue to address this deficiency, we expand our adaptive filter framework to include memreactive components: the memory-capacitor and memory-inductor.<sup>9</sup> These components are described quite similar to the memristor as follows:

$$C_m = C_0 F_C(x_C); \quad \dot{x}_C = f_C(x_C, I_C, t), \quad (3)$$

$$L_m = L_0 F_L(x_L); \quad \dot{x}_L = f_L(x_L, I_L, t). \quad (4)$$

The variables having similar meaning as in Eq. (1) but referring to capacitive and inductive elements, although  $C_m$  and  $L_m$  may not always be passive.<sup>9</sup> We then consider the  $RL_mC_m$  notch filter shown in Fig. 2(a), where the resistor is linear

time-invariant, but the capacitor and inductor have been replaced by their memory-counterparts. Additionally, both of these memreactive components have been demonstrated experimentally,<sup>20,22,23</sup> although in more limited circumstances than memristance, and have also been recently emulated using off-the-shelf electronic components.<sup>24</sup> If the state-variable evolutions  $f_C$  and  $f_L$  are carefully chosen (which in practice amounts to finding or creating the right materials/systems), a circuit can be constructed where the change in  $C_m$  and  $L_m$  “mirror” each other to leave  $\omega_0 = (L_m C_m)^{-1/2}$  constant. This selection requires  $C_m \dot{L}_m + L_m \dot{C}_m = 0$ . The  $Q$  of the notch filter, however, is  $Q = (1/R) \sqrt{L_m/C_m}$ , and thus still changes under the above condition. Because the output magnitude now depends on (nonmemory)  $R$  (instead of  $R_m$  as before),  $V_{\text{out}}(\omega_0)$  will not change. To model the response of such an adaptive-filter in a VO<sub>2</sub> like material, we assign chosen state-variables’ functions as follows:

$$\dot{x}_C = \alpha_C I_C^2, \quad (5)$$

$$\dot{x}_L = \alpha_L I_L^2, \quad (6)$$

$$\alpha_C = -\alpha_L. \quad (7)$$

This straightforward selection allows  $\omega_0$  to remain constant to first order in  $\dot{x}_t$  around the point  $C_0^2 = L_0^2 = \omega_0^{-2}$ . This function also mimics the memristive and memcapactive<sup>20</sup> response in VO<sub>2</sub>, which is understood to be driven by the power through the device and thus is proportional to  $I^2$ .<sup>20</sup> The invariance under  $\pm I$  can be an advantage when designing adaptive filters that respond to ac signals, even though it is understood to be detrimental when considering resettable binary-logic memory. Using these choices, we numerically model a filter similar to the experiment performed above. Again, the small-signal transfer function of the filter is plotted before and after the “A” and “B” pulse sequences used above [Fig. 2(b)]. Pulse A again has little effect on the filter. Pulse B affects an increase in the quality factor  $Q$  by 20%, with a minor accompanying shift in  $\omega_0$  (of 1%). This minor change in  $\omega_0$  is because our chosen forms for  $\dot{x}_C$  and  $\dot{x}_L$  only satisfy  $C_m \dot{L}_m + \dot{L}_m C_m = 0$  to first order. This time, however, the output on-resonance is always self-normalized to  $(V_R/V_{\text{in}}) \times (\omega_0 \approx 72 \text{ Hz}) = 0 \text{ dB m}$ , constructing a filter which may be much easier to work with in practice.

In summary, we have used a vanadium dioxide memristor to demonstrate an adaptive (“learning”) filter. This filter responds preferentially to signals of a specific design frequency by sharpening the quality factor of its bandpass. We also showed how the memreactive components including memory-capacitance and memory-inductance expand the suite of such adaptive filters. As mentioned, it has been shown that simple memristive filters can model the learning patterns observed in biological organisms.<sup>18</sup> As memristive

systems become more common and better understood, circuits such as the above two are likely to find uses in a range of electronics. In particular, we envision filters which initially enable low- $Q$  broad-band detection but self-sharpen as needed when on-resonance signals are present. The analog functionality of memristive components may allow combination of traditional signal processing (such as these bandpass filters) with fuzzy logic and storage, potentially progressing toward the nonlinear analog-digital hybrid mechanisms found in biological systems. When considering potential applications of these types of circuits, it is important to note that although similar adaptive filters may easily be made with combinations of transistors, in the case demonstrated above the circuit consists only of *passive* basic circuit elements. In many situations, it is likely that a single memristive component may be far smaller than the combined active elements needed to emulate this behavior, offering advantages in device density and power consumption.

We acknowledge support from AFOSR and ETRI. M.D. acknowledges partial support from NSF.

<sup>1</sup>J. F. Gibbons and W. E. Beadle, *Solid-State Electron.* **7**, 785 (1964).

<sup>2</sup>W. R. Hiatt and T. W. Hickmott, *Appl. Phys. Lett.* **6**, 106 (1965).

<sup>3</sup>S. R. Ovshinsky, *Phys. Rev. Lett.* **21**, 1450 (1968).

<sup>4</sup>J. Blanc and D. L. Staebler, *Phys. Rev. B* **4**, 3548 (1971).

<sup>5</sup>D. B. Strukov, G. S. Snider, D. R. Stewart, and R. S. Williams, *Nature (London)* **453**, 80 (2008).

<sup>6</sup>J. Joshua Yang, M. D. Pickett, X. Li, D. A. A. Ohlberg, D. R. Stewart, and R. S. Williams, *Nat. Nanotechnol.* **3**, 429 (2008).

<sup>7</sup>L. O. Chua, *IEEE Trans. Circuit Theory* **18**, 507 (1971).

<sup>8</sup>L. O. Chua and S. M. Kang, *Proc. IEEE* **64**, 209 (1976).

<sup>9</sup>M. Di Ventra, Y. V. Pershin, and L. O. Chua, *Proc. IEEE* **97**, 1717 (2009).

<sup>10</sup>R. Colin Johnson, Memristors ready for prime time, EETimes, 07-08-2008, <http://www.eetimes.com/news/design/showArticle.jhtml?articleID=208803176>.

<sup>11</sup>S. Dietrich, *IEEE J. Solid-state Circuits* **42**, 839 (2007).

<sup>12</sup>R. Waser and M. Aono, *Nature Mater.* **6**, 833 (2007).

<sup>13</sup>S. H. Jo, K.-H. Kim, and W. Lu, *Nano Lett.* **9**, 870 (2009).

<sup>14</sup>J. Borghetti, Z. Li, J. Straznicky, X. Li, D. A. A. Ohlberg, W. Wu, D. R. Stewart, and R. Stanley Williams, *Proc. Natl. Acad. Sci. U.S.A.* **106**, 1699 (2009).

<sup>15</sup>S. H. Jo, K.-H. Kim, and W. Lu, *Nano Lett.* **9**, 496 (2009).

<sup>16</sup>Y. V. Pershin and M. Di Ventra, *IEEE Trans. Circuits Syst.* **57**, 1858 (2010).

<sup>17</sup>Y. V. Pershin and M. Di Ventra, *Neural Networks* **23**, 881 (2010).

<sup>18</sup>Y. V. Pershin, S. La Fontaine, and M. Di Ventra, *Phys. Rev. E* **80**, 021926 (2009).

<sup>19</sup>T. Driscoll, H.-T. Kim, B.-G. Chae, M. Di Ventra, and D. N. Basov, *Appl. Phys. Lett.* **95**, 043503 (2009).

<sup>20</sup>T. Driscoll, H.-T. Kim, B.-G. Chae, B.-J. Kim, Y.-W. Lee, N. M. Jokerst, S. Palit, D. R. Smith, M. Di Ventra, and D. N. Basov, *Science* **325**, 1518 (2009).

<sup>21</sup>P. Horowitz and W. Hill, *The Art of Electronics* (Cambridge University Press, Cambridge, England, 1989).

<sup>22</sup>S. Chang, *IEEE Electron Device Lett.* **27**, 905 (2006).

<sup>23</sup>I. Zine-El-Abidine, M. Okoniewski, and J. G. McRory, Proceedings of the International Conference on MEMS, NANO, and Smart Systems (ICMENS’04), 2004, (<http://doi.ieeeecomputersociety.org/10.1109/ICMENS.2004.24>), 636.

<sup>24</sup>Y. V. Pershin and M. Di Ventra, *Electron. Lett.* **46**, 517 (2010).